SLAC-PUB-13168
arXiv:0706.1562v1[astro-ph]

Rapid formation of supermassive black hole binaries in galaxy mergers with gas

L. Mayer,[1,2*] S. Kazantzidis,[3*] P. Madau,[4,5]
M.Colpi,[6] T.Quinn,[7] J. Wadsley[8]

[1]Institut für Astronomie, ETH Zürich, Wolfgang-Pauli-Strasse 16,
CH-8093 Zürich, Switzerland.
[2]Institute for Theoretical Physics, University of Zurich,
Winterthurestrasse 190, CH-8057 Zürich, Switzerland.
[3]Kavli Institute for Particle Astrophysics and Cosmology, Department of Physics,
Stanford University, P.O. Box 20450, MS 29, Stanford,CA 94309 USA.
[4]Department of Astronomy, University of California at Santa Cruz,
1156 High Street, Santa Cruz, CA 95064, USA.
[5]Max Planck Institute für Astrophysik, Karl-Schwarzschild Strasse 1,
85740, Garching bei Muenchen, Germany.
[6]Dipartimento di Fisica, Università di Milano Bicocca,
Piazza della Scienza 3. I-20126 Milano, Italy.
[7]Department of Astronomy, University of Washington,
Stevens Way, Seattle, WA 98195, USA.
[8]Department of Physics and Astronomy, McMaster University,
Hamilton, ON L8S 4M1, Canada.

*To whom correspondence should be addressed; E-mail:
lucio@phys.ethz.ch; stelios@slac.stanford.edu.

Supermassive black holes (SMBHs) are a ubiquitous component of the nuclei of galaxies. It is normally assumed that, following the merger of two massive galaxies, a SMBH binary will form, shrink due to stellar or gas dynamical

Submitted to Science Magazine

Work supported in part by US Department of Energy contract DE-AC02-76SF00515

processes and ultimately coalesce by emitting a burst of gravitational waves. However, so far it has not been possible to show how two SMBHs bind during a galaxy merger with gas due to the difficulty of modeling a wide range of spatial scales. Here we report hydrodynamical simulations that track the formation of a SMBH binary down to scales of a few light years following the collision between two spiral galaxies. A massive, turbulent nuclear gaseous disk arises as a result of the galaxy merger. The black holes form an eccentric binary in the disk in less than a million years as a result of the gravitational drag from the gas rather than from the stars.

Supermassive black holes (SMBHs) weighting up to a billion solar masses are thought to reside at the center of all massive galaxies *(1-3)*. According to the standard paradigm of structure formation in the Universe, galaxies merge frequently as their dark matter halos assemble in a hierarchical fashion *(4,5)*. As SMBHs become incorporated into progressively larger halos, they sink to the center of the more massive progenitor owing to dynamical friction and eventually form a binary *(5-8)*. In a purely stellar background, as the binary separation decays, the effectiveness of dynamical friction slowly declines, and the pair then becomes tightly bound via three-body interactions, namely by capturing stars that pass close to the holes and ejecting them at much higher velocities *(5-7)*. If the hardening continues sufficiently far, the loss of orbital energy due to gravitational wave emission finally takes over, and the two SMBHs coalesce in less than a Hubble time. But the binary may stop sinking before gravitational radiation becomes important since there is a finite supply of stars on intersecting orbits *(5,9)*.

During the assembly of galaxies, however, their SMBHs likely evolve within gas-rich systems. Merging systems like the Ultraluminous Infrared Galaxies (ULIRGs) NGC6240 and Arp220 harbor large concentrations of gas, in excess of 10^9 $M_\odot$, at their center, in the form of either a turbulent irregular structure or of a kinematically coherent, rotating disk*(10-12)*. Mas-

sive rotating nuclear disks of molecular gas are also ubiquitous in galaxies that appear to have just undergone a major merger, such as Markarian 231*(13)*.

Gas dynamics may profoundly affect the pairing of SMBHs both during and after their host galaxies merge*(14-18)*. Recent simulations of the orbital evolution of SMBHs within an equilibrium, rotationally-supported, gaseous disk have shown that friction against the gaseous background leads to the formation of a tightly bound SMBH binary with final separation < 1 pc in about 10^7 yr *(16,17)*. Yet such simulations begin with ad hoc initial conditions, with the black holes already forming a loosely bound pair, while in reality the orbital configuration of the black holes and the structure and thermodynamics of the nuclear region, which can affect the drag *(17-18)*, will be the end result of the complex gravitational and hydrodynamical processes involved in the merger. How a pair of SMBHs binds in a dissipational galaxy merger is thus still unclear.

Here we report on high resolution N-body + smoothed particle hydrodynamics (SPH) simulations of mergers between galaxies with SMBHs having enough dynamic range to follow the holes from a hundred kiloparsecs down to parsec scales, bridging about ten orders of magnitude in density. We start with two equal-mass galaxies similar to the Milky Way, comprising a disk of stars and gas with a surface density distribution that follows an exponential law, a stellar bulge, and a massive and extended spherical dark matter halo whose mass, radius, density profile and angular momentum is consistent with current structure formation models *(19)*. Their initial orbit is parabolic and their distance of closest approach is 50 kpc, consistent with typical values found in cosmological simulations of structure formation*(20)*. A particle of mass $2.6 \times 10^6 M_\odot$ is placed at the center of each bulge to represent a SMBH. The simulations include radiative cooling and star formation *(14)* and have a spatial resolution of 100 pc *(19)*. The computational volume is refined during the late stage of the merger with the technique of particle splitting *(19)*, achieving a spatial resolution of 2 pc with as many as 2×10^6 gas particles within the nuclear

region.

Initially the separation of the two black holes evolves as that of the two gaseous cores in which they are embedded. The galaxies approach each other several times as they sink into one another via dynamical friction. After about 5 Gyr the dark matter halos have nearly merged and the two baryonic cores, separated by about 6 kpc, continue to spiral down (Figure 1). As much as 60% of the gas originally present in the galaxies has been funneled to the inner few hundred parsecs of each core by tidal torques and shocks occurring in the repeated fly-bys between the two galaxies *(14, 21,22)* (Figure 1). Each of the two SMBHs is embedded in a rotating gaseous disk of mass $\sim 4 \times 10^8$ $M_\odot$ and size of a few hundred parsecs, produced by such gas inflow. At this stage we stop the simulation and we restart it with increased resolution *(19)*.

The radiation physics in the refined simulation is modeled via an effective equation of state that accounts for the net balance of radiative heating and cooling. In a previously performed non-refined simulation a starburst with a peak star formation rate of ~ 30 $M_\odot$/yr takes place when the cores finally merge *(14)*. We do not account for any conversion of gas into stars in the refined simulation to limit the computational burden: this will not affect our conclusions since we explore a phase lasting $< 10^7$ yr after the merger, namely much shorter than the duration of the starburst in the non-refined simulation, which is close to 10^8 yr *(19)*. Calculations that include radiative transfer show that the thermodynamic state of a solar metallicity gas heated by a starburst can be well approximated by an ideal gas with adiabatic index $\gamma = 1.3 - 7/5$ over a wide range of densities *(23,24)*. We assume $\gamma = 7/5$ and include the irreversible heating generated by shocks via an artificial viscosity term in the internal energy equation *(19)*.

The gaseous cores finally merge at $t \sim 5.12$ Gyr, forming a single nuclear disk with a mass of $3 \times 10^9 M_\odot$ and a size of ~ 75 pc. The two SMBHs are now embedded in such nuclear disk. The disk is more massive than the sum of the two progenitor nuclear disks formed earlier because further gas inflow occurs in the last stage of the galaxy collision. It is surrounded by

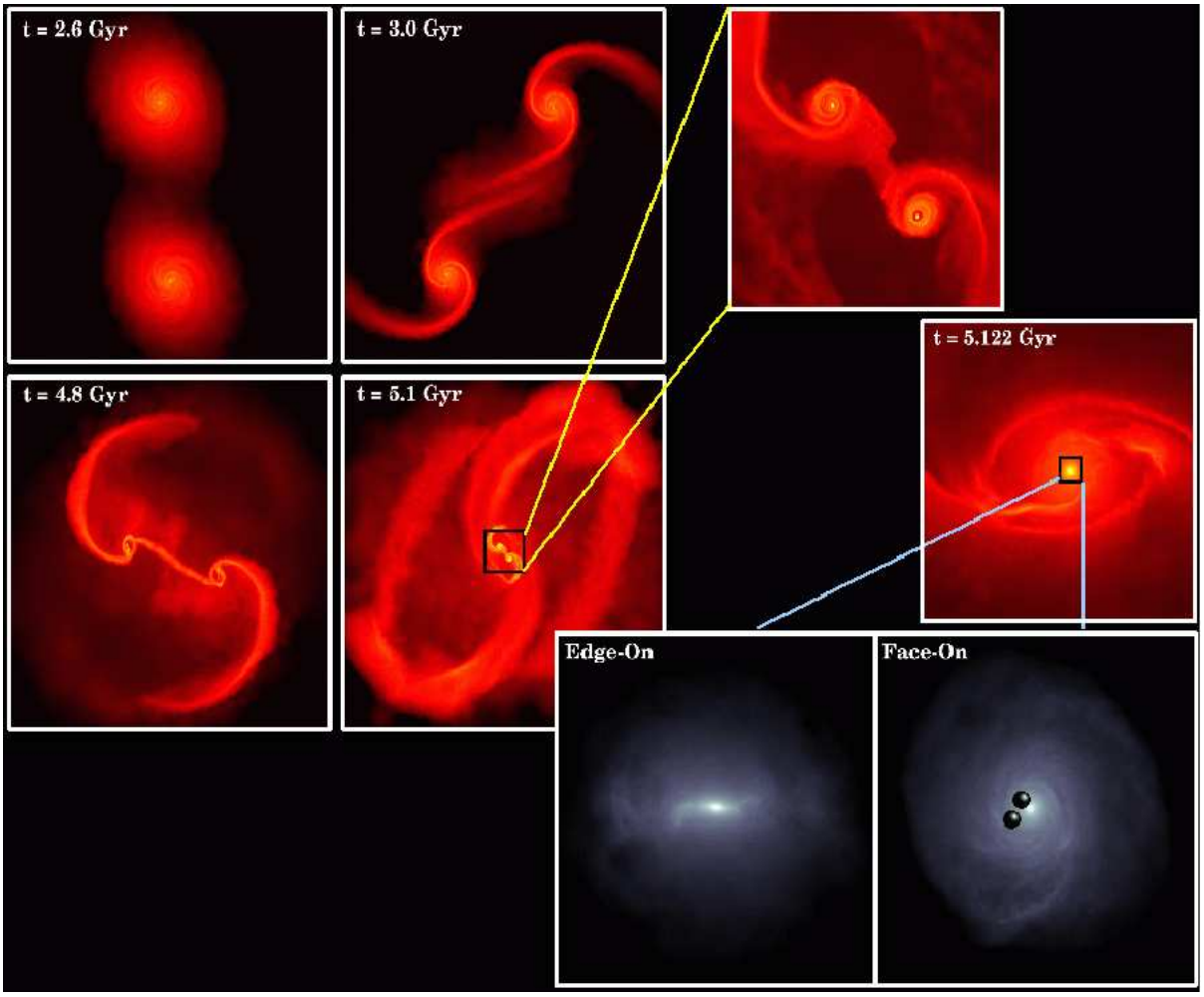

Figure 1: The different stages of the merger between two identical disk galaxies. The color coded density maps of the gas component are shown using a logarithmic scale, with brighter colors for higher densities. The four panels to the left show the large-scale evolution at different times. The boxes are 120 kpc on a side (top) and 60 kpc on a side (bottom) and the density ranges between 10^{-2} atoms cm^{-3} and 10^{2} atoms cm^{-3}. During the interaction tidal forces tear the galactic disks apart, generating spectacular tidal tails and plumes. The panels to the right show a zoom in of the very last stage of the merger, about 100 million years before the two cores have fully coalesced (upper panel), and 2 million years after the merger (middle panel), when a massive, rotating nuclear gaseous disk embedded in a series of large-scale ring-like structures has formed. The boxes are now 8 kpc on a side and the density ranges between 10^{-2} atoms cm^{-3} and 10^{5} atoms cm^{-3}. The two bottom panels, with a grey color scale, show the detail of the inner 160 parsecs of the middle panel; the nuclear disk is shown edge-on (left) and face-on (right), and the two black holes are also shown in the face-on image. An equation of state with $\gamma = 7/5$ was used in the refined part of the simulation.

several rings and by a more diffuse, rotationally-supported envelope extending out to more than a kiloparsec from the center (Figure 1). A background of dark matter and stars distributed in a spheroid is also present but the gas component is dominant in mass within a few hundred pc from the center. From now on the orbital decay of the holes is dominated by dynamical friction against the gaseous disk. The black holes are on eccentric orbits (the eccentricity is $e \sim 0.5$ where $e = (r_{\rm apo} - r_{\rm peri})/(r_{\rm apo} + r_{\rm peri})$, $r_{\rm apo}$ and $r_{\rm peri}$ being, respectively, the apocenter and pericenter of the orbit) near the plane of the disk *(19)*, and move at a speed $v_{\rm BH} \sim 200 - 300$ km s^{-1} relative to the disk's center of mass. The typical ambient sound speed is $v_s \sim 45$ km s^{-1}, a legacy of the strong shock heating occurring as the galaxy cores merge. The disk is rotationally supported, $v_{\rm rot} \sim 300$ km s^{-1}, but is also highly turbulent, having a typical velocity dispersion $v_{\rm turb} \sim 100$ km s^{-1}*(19)*. Its scale height, ~ 20 pc, and typical density, $10^3 - 10^4$ atoms cm^{-3}, are comparable to those of observed nuclear disks *(11)*.

The two SMBHs sink down from about 40 pc to a few parsecs, our resolution limit, in less than a million years (Figure 2). At this point the two holes are gravitationally bound to each other, as the mass of the gas enclosed within their separation is less than the mass of the binary. The gas controls the orbital decay, not the stars. Dynamical friction against the stellar background would bring the two black holes this close only on a much longer timescale, $\sim 5 \times 10^7$ yr *(19)*. A short sinking timescale due to the gas is expected because of the high gas densities and since the decay occurs in the supersonic regime *(19)*, being $v_{\rm BH} > v_{\rm turb} > v_s$. The subsequent hardening of the binary will depend on the details of gasdynamics and other processes at scales below our resolution *(16-19)*.

If radiative cooling is completely suppressed during the merger, for example as a result of radiative heating following gas accretion onto the SMBHs, the gas would evolve adiabatically ($\gamma = 5/3$). In this case the hardening process is significantly slowed down, and gas and stars contribute similarly to the drag *(19)*. However, if the SMBHs become active only after the

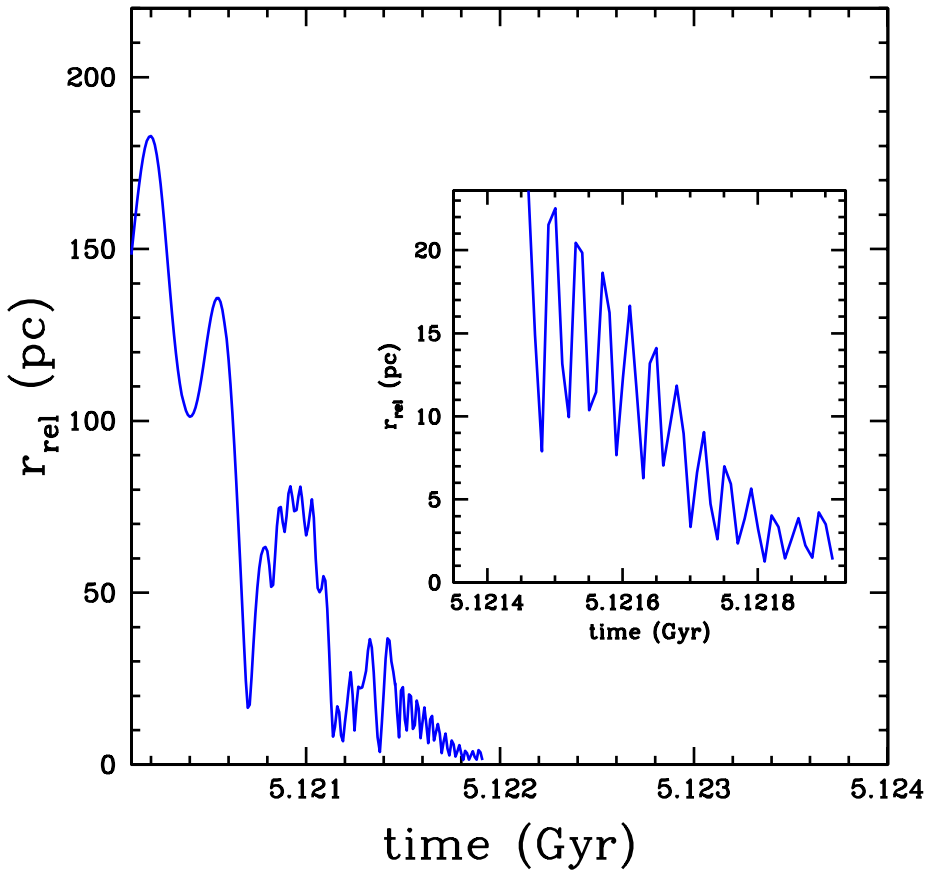

Figure 2: Orbital separation of the two black holes as a function of time during the last stage of the galaxy merger shown in Figure 1. The orbit of the pair is eccentric until the end of the simulation. The two peaks at scales of tens of parsecs at around $t = 5.1213$ Gyr mark the end of the phase during which the two holes are still embedded in two distinct gaseous cores. Until this point the orbit is the result of the relative motion of the cores combined with the relative motion of each black hole relative to the surrounding core, explaining the presence of more than one orbital frequency. The inset shows the details of the last part of the orbital evolution, which takes place in the nuclear disk arising from the merger of the two cores. The binary stops shrinking when the separation approaches the softening length (2 pc).

nuclear disk arises and keep accreting the surrounding gas at the Eddington limit until the binary forms, their radiative heating should not be enough to alter significantly the energy balance implicitly assumed in the $\gamma = 7/5$ simulation (19).

Here we have considered a merger between galaxies in which the gas accounts for only 10% of the disk mass, a typical gas fraction in present-day spirals. Much larger gas fractions should be common at high redshift, when most of the merger activity takes place and massive galaxies have just begun to assemble their stellar component*(25)*. Even more massive and denser nuclear disks should form then and, since dynamical friction is proportional to the density of the background *(16,19)*, a pair of SMBHs will bind even faster than in our calculations. Coalescing SMBH binaries will thus be common at high redshift and are among the primary candidate sources of gravitational waves at mHz frequencies, the range probed by the space-based Laser Interferometer Space Antenna (LISA)*(7,26)*. Moreover, even at the present epoch a typical bright galaxy has a more massive stellar bulge relative to our models, and hence harbors more massive SMBHs *(1-3)* that will decay faster because dynamical friction is stronger for larger bodies.

Three-body encounters between ambient stars and a SMBH binary may deplete the nuclear region and turn a stellar cusp into a low-density core at scales of tens of parsecs *(27)*. This would explain why the brightest ellipticals, very likely the end result of several mergers, have shallow stellar cores *(28, 29)*. In our scenario the orbital decay is driven by the gas rather than by the stellar background and occurs on such a short timescale that the interaction between the binary and the stellar spheroid would be negligible and should hardly affect the stellar density profile. Gas-rich mergers yield steep stellar profiles owing to the dramatic gas inflow and subsequent star formation *(21)*. We expect that such cuspy profiles will be preserved in the remnant because of the negligible interaction between the binary SMBHs and the stars implied by our calculations. Remnants of dissipational mergers such as Markarian 231 *(13)* do indeed

exhibit a steep stellar profile at least down to a hundred parsecs, and a small effective radius reminiscent of that of low-luminosity ellipticals galaxies that have cuspy profiles down to a few parsecs *(28)*. Our prediction can be thoroughly tested with current and future high resolution multi-wavelength observations capable of probing the inner few parsecs of the remnants of dissipational mergers.

References and Notes

1. Kormendy, J. & Richtsone, D., *Ann. Rev. Astron. Astrophys.* **33**, 581 (1995)
2. Richtsone, D., *et al.*, *Nature*, **3**95, A14 (1998)
3. Tremaine, S. et al., *Astrophys. J.*, **574**, 740 (2002)
4. Springel, V., *et al.*, *Nature*, **435**, 629 (2006)
5. Volonteri, M., Haardt, F. & Madau, P., *Astrophys. J.*, **582**, 559 (2003)
6. Begelman, M. C., Blandford, R. D. & Rees, M. J., *Nature* **287**, 307, (1980)
7. Milosavljevic, M. & Merritt, D.,*Astrophys. J.*, **563**, 34 (2001)
8. Sesana, A., Haardt, F., Madau., P. & Volonteri, M., *Astrophys. J.*, **611**, 23 (2005)
9. Berczik, P., Merritt, D., Spurzem, R., & Bischof, H., *Astrophys. J*. **633**, 680, (2005)
10. Greve, T.R., Papadopoulos, P.P., Gao, Y., & Radford, S.J.E., submitted to Astrophys. J. (2006) (astro-ph/0610378)
11. Downes, D. & Solomon, P. M.,*Astrophys. J.*, **507**, 615 (1998)
12. Davies, R. I., Tacconi, L. J. & Genzel, R.*Astrophys. J.*, **602**, 148 (2004)

13. Davies, R. I., Tacconi, L. J. & Genzel, R. *Astrophys. J.*, **613**, 781 (2004)

14. Kazantzidis, S., Mayer, L., Colpi, M., Madau, P., Debattista, V., Quinn, T., Wadsley, J. & Moore, B.,*Astrophys. J.*, **623**, L67 (2005)

15. Escala, A., Larson, R. B., Coppi, P. S., & Mardones, D., *Astrophys. J.*, **607**, 765 (2004)

16. Escala A., Larson, R. B., Coppi, P. S. & Mardones, D., *Astrophys. J.*, **630**, 152 (2005)

17. Dotti, M., Colpi, M. & Haardt, F.*Mon. Not. R. Astron. Soc.*, **367**, 103 (2006)

18. Ostriker, E., *Astrophys. J.*, **513**, 252 (1999)

19. Material and Methods are available as supporting material on *Science* online.

20. Khochfar, S. & Burkert, A., *Astron. Astrophys.*, **445**, 403 (2006)

21. Barnes, J. & Hernquist, L., *Astrophys. J.*, **471**, 115 (1996)

22. Springel, V., Di Matteo, T., & Hernquist, L., *Mon. Not. R. Astron. Soc.*, **361**, 776 (2005)

23. Spaans, M. & Silk, J., *Astrophys. J.*, **538**, 115 (2000)

24. Klessen, R.S., Spaans, M., Jappsen, A., *Mon. Not. R. Astron. Soc.*, **374**, L29 (2007)

25. Genzel, R., *et al.*, *Nature*, **442**, 786 (2005)

26. Cutler, C. & Thorne, K.S., *Proceedings of GR16* (Durban, South Africa) (2002)

27. Merritt, D., *Astrophys. J.*, **6**48, 976 (2006)

28. Lauer, T.R. *et al.*,*Astronom. J.*, **1**10, 2622 (1995)

29. Graham, A. W., *Astrophys. J.*, **6**13, L33 (2004)

30. We acknowledge discussions with Marcella Carollo, Massimo Dotti, Andres Escala, Savvas Koushiappas, David Merritt, Rainer Spurzem, Monica Valluri, and Marta Volonteri S.Kazantzidis is funded by the U.S. Department of Energy through a KIPAC Fellow ship at Stanford University and the Stanford Linear Accelerator Center. P. Madau acknowledges support by NASA and by the Alexander von Humboldt Foundation. All simulations were performed on Lemieux at the Pittsburgh Supercomputing Center, on the Zbox and Zbox2 supercomputers at the University of Zürich, and on the Gonzales cluster at ETH Zürich.

Supporting Online Material

Material and Methods

SOM text

Figs:S1 to S5

SUPPORTING ONLINE MATERIAL

Here we briefly describe the setup of the initial conditions and the numerical methods used to perform the simulations presented in the Letter along with resolution tests. This is followed by a critical discussion of the assumptions behind the modeling of thermodynamics in the simulations. With the aid of additional numerical experiments we also explore how the structure of the nuclear region and the sinking time of the black holes depend on thermodynamics.

1 Numerical Methods

1.1 The N-Body+SPH code:GASOLINE

We have used the fully parallel, N-Body+smoothed particle hydrodynamics (SPH) code GASOLINE to compute the evolution of both the collisionless and dissipative component in the simulations. A detailed description of the code is available in the literature($S1$). Here we recall its essential features. GASOLINE computes gravitational forces using a tree–code($S2$) that employs multipole expansions to approximate the gravitational acceleration on each particle. A tree is built with each node storing its multipole moments. Each node is recursively divided into smaller subvolumes until the final leaf nodes are reached. Starting from the root node and moving level by level toward the leaves of the tree, we obtain a progressively more detailed representation of the underlying mass distribution. In calculating the force on a particle, we can tolerate a cruder representation of the more distant particles leading to an $O(N \log N)$ method. Since we only need a crude representation for distant mass, the concept of "computational locality" translates directly to spatial locality and leads to a natural domain decomposition. Time integration is carried out using the leapfrog method, which is a second-order symplectic integrator requiring only one costly force evaluation per timestep and only one copy of the physical state of the system.

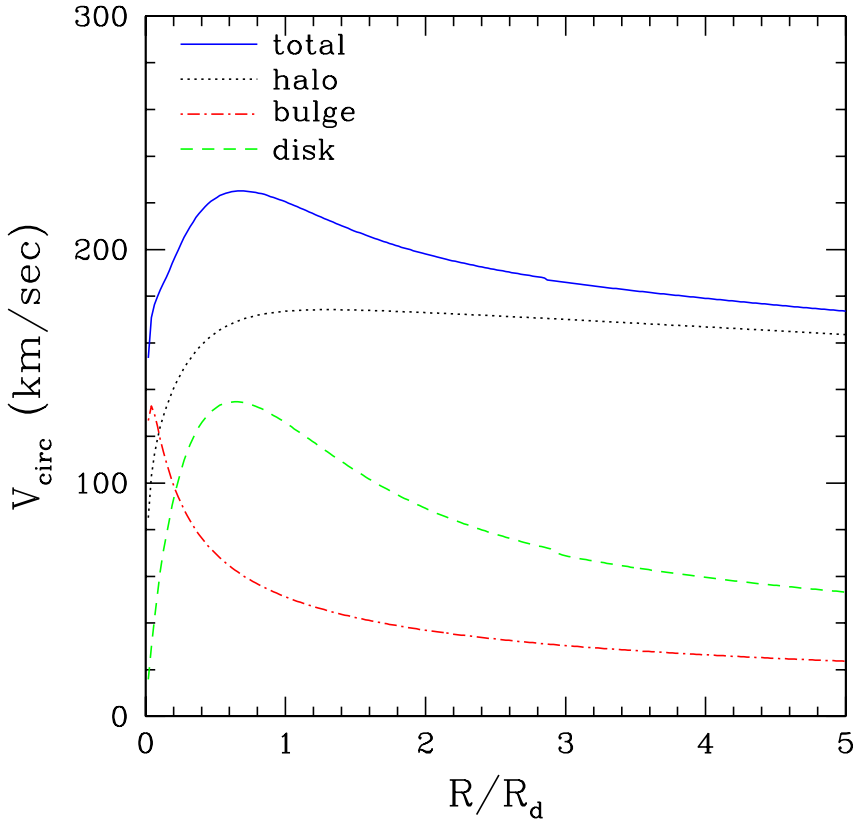

Figure S1. Rotation curve of the multi-component galaxy model used in the merger simulation. The different lines represent the contribution of the different component of the galaxy to the total rotation curve (blue line) as indicated in the Figure.

SPH is a technique of using particles to integrate fluid elements representing gas$(S3, S4)$ GASOLINE is fully Lagrangian, spatially and temporally adaptive and efficient for large N. It employs radiative cooling in the galaxy merger simulation used as a starting point for the refined simulations presented in this Report. We use a standard cooling function for a primordial mixture of atomic hydrogen and helium. We shut off radiative cooling at temperatures below 2×10^4 K that is about a factor of 2 higher than the temperature at which atomic radiative cooling would drop sharply due to the adopted cooling function. With this choice we take into account non-thermal, turbulent pressure to model the warm ISM of a real galaxy$(S5)$. Unless strong shocks occur (this will be the case during the final stage of the merger) the gaseous disk evolves nearly isothermally since radiative cooling is very efficient at these densities (< 100 atoms/cm^3) and temperatures (10^4 K), and thus dissipates rapidly the compressional heating resulting from the non-axisymmetric structures (spiral arms, bars) that soon develop in each

galaxy as a result of self-gravity and the tidal disturbance of the companion. The cooling rate would increase with the inclusion of metal lines, but $(S31)$ have shown that the equation of state of gas at these densities is still nearly isothermal ($\gamma \sim 0.9 - 1.1$) for a range of metallicities (with γ being lower for higher metallicity), supporting the validity of simple choice for the cooling function. Cooling by metals will surely be important below 10^4 K, but this would be irrelevant in our scheme since we have imposed a temperature floor of 2×10^4 K to account for non-thermal pressure (see above). The specific internal energy of the gas is integrated using the asymmetric formulation. With this formulation the total energy is conserved exactly (unless physical dissipation due to cooling processes is included) and entropy is closely conserved away from shocks, which makes it similar to alternative entropy integration approaches$(S6)$. Dissipation in shocks is modeled using the quadratic term of the standard Monaghan artificial viscosity$(S4)$. The Balsara correction term is used to reduce unwanted shear viscosity$(S7)$. The galaxy merger simulation$(S8)$ includes star formation as well. The star formation algorithm is such that gas particles in dense, cold Jeans unstable regions and in convergent flows spawn star particles at a rate proportional to the local dynamical time$(S9, S10)$. The star formation efficiency was set to 0.1, which yields a star formation rate of $1-2M_{\odot}$/yr for models in isolation that have a disk gas mass and surface density comparable to those of the Milky Way.

1.2 The simulations of galaxy mergers

For the Report we performed a refined calculation of a galaxy merger simulation between two identical galaxies. The initial conditions of this and other similar merger simulations are described in a previous paper$(S8)$. We employed a multicomponent galaxy model constructed using the technique originally developed in $(S11, S12)$, its structural parameters being consistent with the ΛCDM paradigm for structure formation$(S13)$. The model comprises a spherical and isotropic Navarro-Frenk-and-White (NFW) dark matter (DM) halo$(S14, S15)$, an expo-

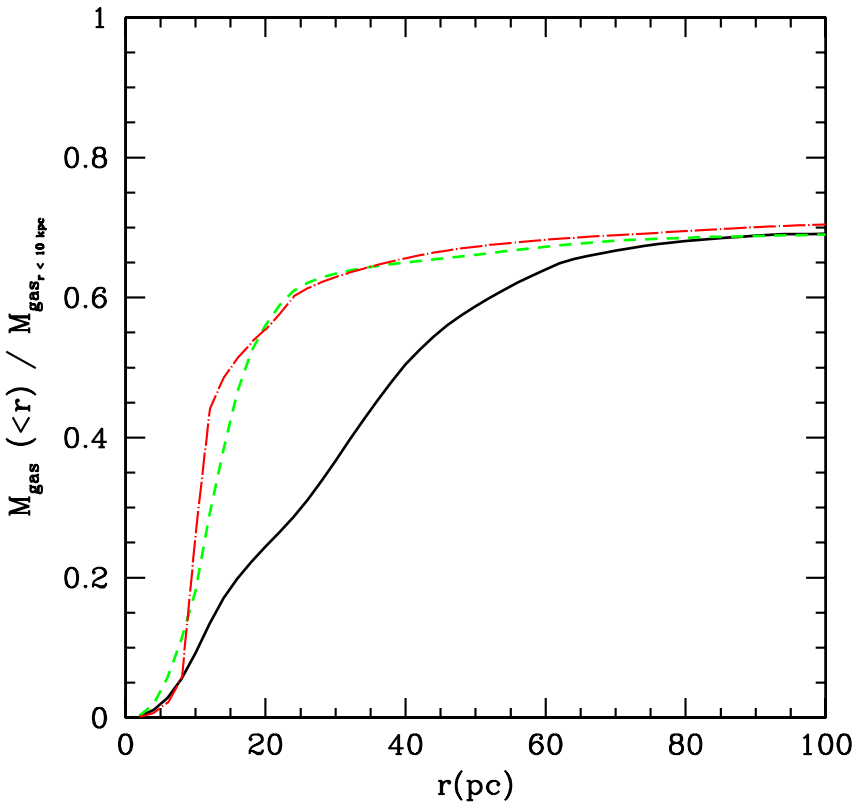

Figure S2. Cumulative gas mass profile (normalized to the total gas mass) within the inner 100 pc. Three simulations with $\gamma = 7/5$ for three different values of the gravitational softening are shown, 40 pc (black solid line), 10 pc (red dot-dashed line) and 2 pc (green dashed line).

nential disk, and a spherical, non-rotating bulge. We adopted parameters from the Milky Way model A1 of $(S16)$. Specifically, the DM halo has a virial mass of $M_{\rm vir} = 10^{12} M_{\odot}$, a concentration parameter of $c = 12$, and a dimensionless spin parameter of $\lambda = 0.031$. The mass, thickness and resulting scale length of the disk are $M_{\rm d} = 0.04 M_{\rm vir}$, $z_0 = 0.1 R_{\rm d}$, and $R_{\rm d} = 3.5$ kpc, respectively. The bulge mass and scale radius are $M_{\rm b} = 0.008 M_{\rm vir}$ and $a = 0.2 R_{\rm d}$, respectively. The DM halo was adiabatically contracted to respond to the growth of the disk and bulge$(S17)$ resulting in a model with a central total density slope close to isothermal. The galaxies are consistent with the stellar mass Tully-Fisher and size-mass relations. To each of them we add a (softened) particle initially at rest at the center of the bulge to represent a supermassive black hole (SMBH). We used a SMBH mass equal to $M_{\rm BH} = 2.6 \times 10^6 M_{\odot}$, consistent with the $M_{BH} - \sigma$ relation$(S8)$.

The gas fraction, $f_{\rm g}$, is 10% of the total disk mass. The rotation curve of the model is shown

in Figure S1. Different encounter geometries were explored in the large suite of merger simulations previously performed and published($S15$): prograde or retrograde coplanar mergers as well as mergers in which one of the disks was inclined with respect to the orbital plane. The simulation presented in this Report is the refined version of a coplanar prograde encounter. This particular choice is by no means special for our purpose, except that the galaxies merge slightly faster than in the other cases, thus minimizing the computational time invested in the expensive refined simulation. We note that the existence of a coherent nuclear disk after the merger is a general result that does not depend on the details of the initial orbital configuration, including the initial relative inclination of the two galaxies($S15$). Similarly, gas masses and densities in the nuclear region differ by less than a factor of 2 for runs having the same initial gas mass fraction in the galaxy disks but different initial orbits.

The galaxies approach each other on parabolic orbits with pericentric distances that were 20% of the galaxy's virial radius, typical of cosmological mergers($S18$) . The initial separation of the halo centers was twice their virial radii and their initial relative velocity was determined from the corresponding Keplerian orbit of two point masses. Each galaxy consists of 10^5 stellar disk particles, 10^5 bulge particles, and 10^6 DM particles. The gas component was represented by 10^5 particles. We adopted a gravitational softening of $\epsilon = 0.1$ kpc for both the DM and baryonic particles of the galaxy, and for its SMBH $\epsilon = 0.03$ kpc.

1.3 The refined simulations of the nuclear region

1.3.1 Particle splitting

In this Report we use the same technique of particle splitting that we have used before to study the formation of a disk galaxy($S19$). Splitting has been already used to follow supermassive black holes evolving in spherical gaseous backgrounds($S20$) and to model the formation of primordial stars and black holes at high redshift($S21$).Several schemes for particle splitting have

been proposed , both static and dynamic, and it has been shown that splitting gives robust results even when simulating highly dynamical systems such as collapsing clouds($S22$). In dynamic splitting the mass resolution is increased during the simulation based on some criterion, such as the local Jeans length of the system. This requires extreme care when calculating SPH density or pressure at the boundary between the fine grained and the coarse grained volumes. In static splitting the approach is much more conservative and one simply selects a subvolume to refine. The simulation is then restarted with increased mass resolution just in the region of interest. We adopted the latter technique. By selecting a large enough volume for the fine grained region one can avoid dealing with spurious effects at the coarse/fine boundary. We select the volume of the fine-grained region large enough to guarantee that the dynamical timescale of the entire coarse-grained region is much longer than the dynamical timescale of the refined region. In other words, we make sure that gas particles from the coarse region will reach the fine region on a timescale longer than the actual time span probed in this work. This is important because the more massive gas particles from the coarse region can exchange energy with the lower mass particles of the refined region via two-body encounters, artificially affecting their dynamics and thermodynamics($S20, S23$). Hence our choice to split in a volume of 30 kpc in radius, while the two galaxy cores are separated by only 6 kpc. The new particles are randomly distributed according to the SPH smoothing kernel within a volume of size $\sim h_p^3$, where h_p is the smoothing length of the parent particle. The velocities of the child particles are equal to those of their parent particle (ensuring momentum conservation) and so is their temperature, while each child particle is assigned a mass equal to $1/N_{\rm split}$ the mass of the parent particle, where $N_{\rm split}$ is the number of child particles per parent particle. The mass resolution in the gas component was originally $2 \times 10^4 M_\odot$ and becomes $\sim 3000 M_\odot$ after splitting, for a total of 1.5 million SPH particles.. The star and dark matter particles are not splitted to limit the computational burden. The softening of the gas particles is reduced to 2 pc (it was 100 pc in the low resolution simu-

lations). For the new mass resolution, the local Jeans length is always resolved by 10 or more SPH smoothing kernels$(S24\,, S25)$ in the highest density regions occurring in the simulations. The softening of the black holes is also reduced from 30 pc to 2 pc. The softening of dark matter and star particles remains 100 pc because they are not splitted. Therefore in the refined simulations stars and dark matter particles essentially provide a smooth background potential to avoid spurious two-body heating against the much lighter gas particles, while the computation focuses on the gas component which dominates by mass in the nuclear region (see sections 2.1-2.3). We have verified that, thanks to the fact that gas dominates the mass and dynamics of the nuclear region, the large softening adopted for the dark matter particles does not affect significantly the density profile of the inner dark halo that surrounds the nuclear disk. We constructed an equilibrium gaseous disk embedded in a dark halo choosing parameters as close as possible to the nuclear disk of the merger remnant in our simulation. The mass ratio between the equilibrium disk and the dark halo is a factor of 2 lower than that in our simulation in order to facilitate the stability of the disk against fragmentation in absence of turbulence (turbulence is a significant stabilizing factor in the merger remnant of our standard simulation). We evolve the system with different particle numbers and choosing a softening of the dark matter particles as large as the disk radius, as in the refined simulations, or 30 times smaller, i.e. equal to that of the gas particles. We compare the different runs after evolving the gaseous disk for a few orbital times and we find that spurious effects are seen in the profiles of the large dark matter softening simulation only at scales as small as 3-4 times the softening of the gas particles (Figure S3). At such distance from the center the density profile flattens out and is about a factor of 3 lower than in the simulation with small dark matter softening. The reason why a flattening of the density profile does not occur at a much larger scale of order the dark matter softening is because gas dominates the inner mass distribution, causing a contraction of the halo that overwhelms the tendency to form a constant density core owing to the large softening (the effect of

halo contraction on the slope of density profiles is recognized to be important in general and has been widely studied and demonstrated, even in the context of mergers $(S8)$). Moreover, the total density profile, including the gas component, is even less affected (Figure S3). The total density profile is actually most relevant for the overall strength of dynamical friction. In summary, the effect of the large dark matter softening is only manifest at scales that approach the nominal resolution of the simulation set by the gas softening and therefore it hardly affects the sinking of the black hole pair.

1.3.2 Resolution tests

In fluid systems for which gravity plays a major role, as it is the case here, the effective spatial resolution is set by the largest between the gravitational softening and the SPH smoothing length. These can be forced to be always equal, such as in experiments of molecular cloud collapse$(S26)$, but this requires introducing adaptive gravitational softening, which can cause spurious fluctuations in the potential energy of the particles. Here we opt for a fixed gravitational softening$(S8)$ and we set it in such a way as to have a high force resolution while being comparable or somewhat larger than the SPH smoothing length (or, more precisely, a spherical volume of radius equal to the softening always contains of order $2 * N_{\rm sph}$ or more, where $N_{\rm sph}$ is the number of neighboring particles used in the SPH calculation (=32 in GASOLINE).

The latter choice avoids spurious fragmentation$(S24\,, S25)$. During the late stage of the merger densities grow considerably, and locally the SPH smoothing lengths can be appreciably smaller than the softening, with the result that the radial inflow of gas might be suppressed, as in the analogous case of star forming clouds$(S24)$. We tested how the results depend on the choice of the gravitational softening of the gas by running the refined part of the calculation with a softening of 40 pc, 10 pc, or 2 pc (the latter is our choice in the reference simulation used in the Report). We adopt an adiabatic equation of state with $\gamma = 7/5$ (see next section). We

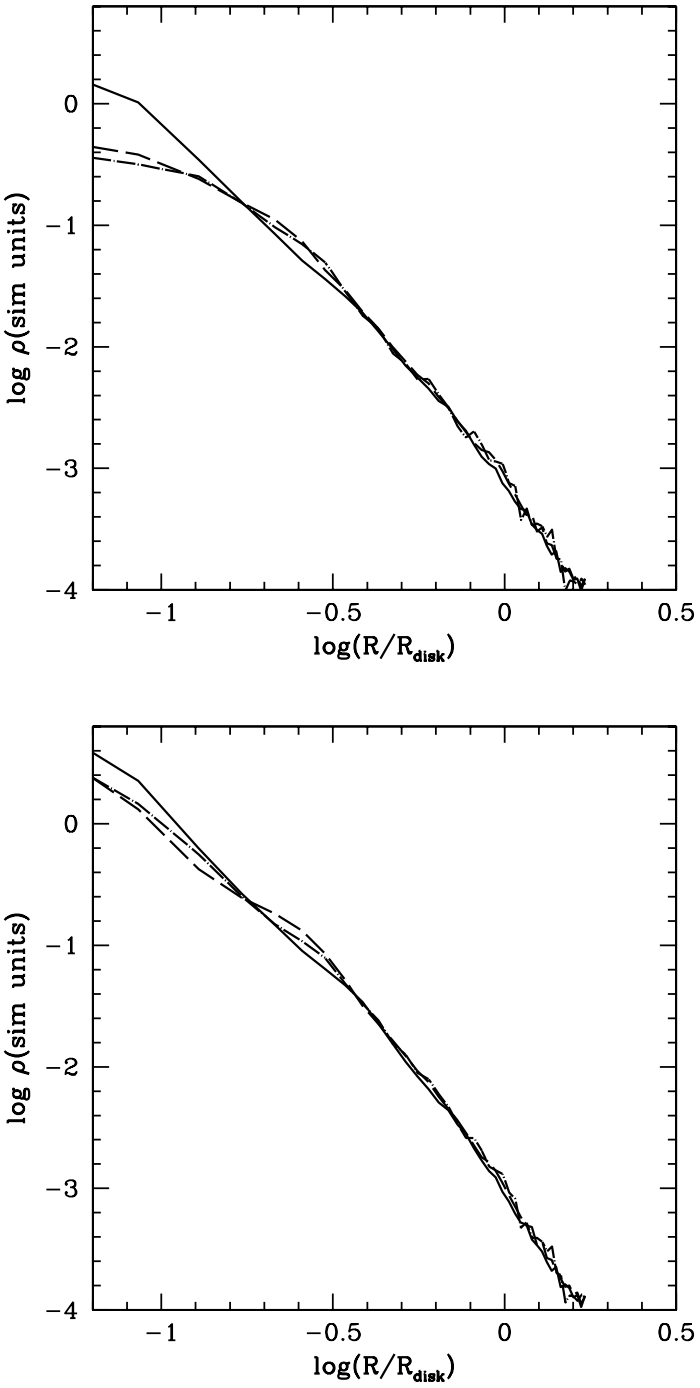

Figure S3. Density profiles of the dark matter (top) and of the sum of the dark matter and gaseous component (bottom) of an equilibrium nuclear gaseous disk embedded in a dark matter halo ($R_{\rm disk}$ is the radius of the nuclear disk and the density is measured in simulation units). The tests were run to study the dependence of the profiles on the softening of the dark matter component (see 1.3.1 for a description of the test). Different curves correspond to different simulations. The solid line is used for a simulation with a dark matter softening $= 0.033R_{\rm disk}$ and 50000 particles in the halo, the dashed line refers to a simulation with a dark matter softening equal to R_{disk} and 50000 halo particles, and the dot-dashed line is used for a simulation with a dark matter softening equal to $R_{\rm disk}$ and 5000 halo particles. In all simulations the softening of the gas is $= 0.033R_{\rm disk}$. The curves are shown from two gas softening lengths outwards..

find that the gas mass profile at scales smaller than 100 pc, namely in the region of the nuclear disk, approaches convergence at a softening of about 10 pc (see Figure S2). This means that the amount of gas that ends up in the nuclear disk, which ultimately determines the strength of the drag, is a robust result (see also 2.2). Likewise, the scale height and global structural properties of the nuclear disk, such as average density, size, sound speed, velocity dispersion and rotational velocity are nearly equal when comparing the 10 pc and the 2 pc runs. This explains why the orbital decay rate is nearly identical until the two SMBHs are separated by a distance resolved with both the 10 pc an the 2 pc simulation($S27$). On the other end, the non-axisymmetric features in the disk and the gas inflow at the smallest scales become increasingly better resolved as the gravitational softening is decreased, implying that an even higher resolution will be necessary to study the fueling of the black holes in a robust way.

1.4 Thermodynamics of the nuclear region: the model

In the refined simulations the gas is ideal and each gas particle obeys $P = (\gamma - 1)\rho u$. The specific internal energy u evolves with time as a result of PdV work and shock heating modeled via the standard Monaghan artificial viscosity term (no explicit radiative cooling term is included). We refer to section 1.1 for a description of the implementation.

The entropy of the system increases as a result of shocks. Including irreversible heating from shocks is important in these simulations since the two galaxy cores undergo a violent collision. Shocks are generated even later as the nuclear, self-gravitating disk becomes non-axisymmetric, developing strong spiral arms. Therefore the highly dynamical regime modeled here is much different from that considered by previous works starting from an equilibrium disk model, which could be evolved using a polytropic equation of state and neglecting shock heating($S28 - S30$). Radiative cooling is not directly included in the refined simulations. Instead, the magnitude of the adiabatic index, namely the ratio between specific heats, is changed

in order to mimic different degrees of dissipation in the gas component, thereby turning the equation of state of the gas into an "effective" equation of state($S26$, $S31$, $S32$).

Previous works($S31$) have used a two-dimensional radiative transfer code to study the effective equation of state of interstellar clouds exposed to the intense UV radiation field expected in a starburst finding that the gas has an adiabatic index γ in the range $1.3 - 1.4 (= 7/5)$ for densities in the range $5 \times 10^3 - 5 \times 10^4$ atoms/cm^3. The latter density is comparable to the volume-weighted mean density in our simulated nuclear disks. Such values of the adiabatic index are expected for quite a range of starburst intensities, from $10\ M_\odot$/yr to more than $100\ M_\odot$/yr($S32$), hence encompassing the peak star formation rate of $\sim 40 M_\odot$/yr measured in the original galaxy merger simulations(8). Hence under these conditions the nuclear gas is far from isothermal ($\gamma = 1$), which would correspond to radiative cooling being so efficient to balance heating coming from compression and/or radiative processes, as it happens in the first stage of the simulation. The inefficient cooling is mostly due to a high optical depth which causes trapping of H_2O lines. In addition the warm dust heated by the starburst continuously heats the gas via dust-gas collisions, and the cosmic-rays also heat the gas substantially. We adopt $\gamma = 7/5$ in the simulation described in the Report (we have also run a case for $\gamma = 1.3$ and found that the structure of the nuclear disk is substantially unchanged). In essence, we treat the gas as a one-phase medium whose mean density and internal energy (the sum of thermal and turbulent energy) will correspond to the mean density and line width seen in observed nuclear disks($S33$).

In section 2.2 we provide more details on the structure of the nuclear disk. For densities above 10^5 atoms/cm^3 or below 10^3 atoms/cm^3 cooling is more efficient and γ should drop even below 1($S31$) Therefore, in reality the nuclear disks will have a complex multi-phase structure with temperatures and densities spanning orders of magnitude, as shown by detailed numerical calculations($S34$, $S35$). In particular, the lowest density and highest density gas present in the

refined simulation would be characterized by have an effective sound speed, $v_s = \sqrt{\gamma k_B T/\mu}$, lower than that in the simulation. A lower gas sound speed will yield a faster decay of the black hole binary($S28$). This is because the drag is more efficient in a supersonic rather than in a subsonic regime($S36$). Since the gas in the simulation is already transonic the sound speed need not be much lower for the gas to become supersonic. A colder gas will also becomes denser, which again goes in the direction of increasing the sinking rate of the black holes. Hence, if anything we err on the side of underestimating the drag by using a constant, high γ everywhere. A faster decay will only strengthen our scenario.

We tested that the transition between the thermodynamical scheme used in the low-res part of the simulation, which adopts the cooling function described in section 1.1, and the second thermodynamical scheme with the effective equation of state does not introduce large fluctuations in the hydrodynamical variables. This was done by rerunning the refined stage of the simulation with the same cooling function adopted in the low resolution part of the simulation. This new refined simulation was then compared with the standard $\gamma = 7/5$ refined simulation before the merger, just one crossing time of the inner region (calculated within a volume of 200 pc around one of the cores) after refinement. We recall that in the standard simulations we introduce the effective equation of state exactly when we apply the refinement. The chosen time is shorter than the merging time of the two cores but long enough to show eventual fluctuations resulting from switching to the effective equation of state in our standard refined simulation. We find that the density distributions are nearly identical in the cores, while they are slightly different in the region of high compression between the two cores. Such differences are of the expected sign, namely that a larger pressure gradient develops with the effective equation of state compared to the cooling simulation as the two disks approach each other (indeed the refined simulation with cooling behaves almost as an isothermal run, i.e. corresponds to a softer equation of state relative to the $\gamma = 7/5$ run).

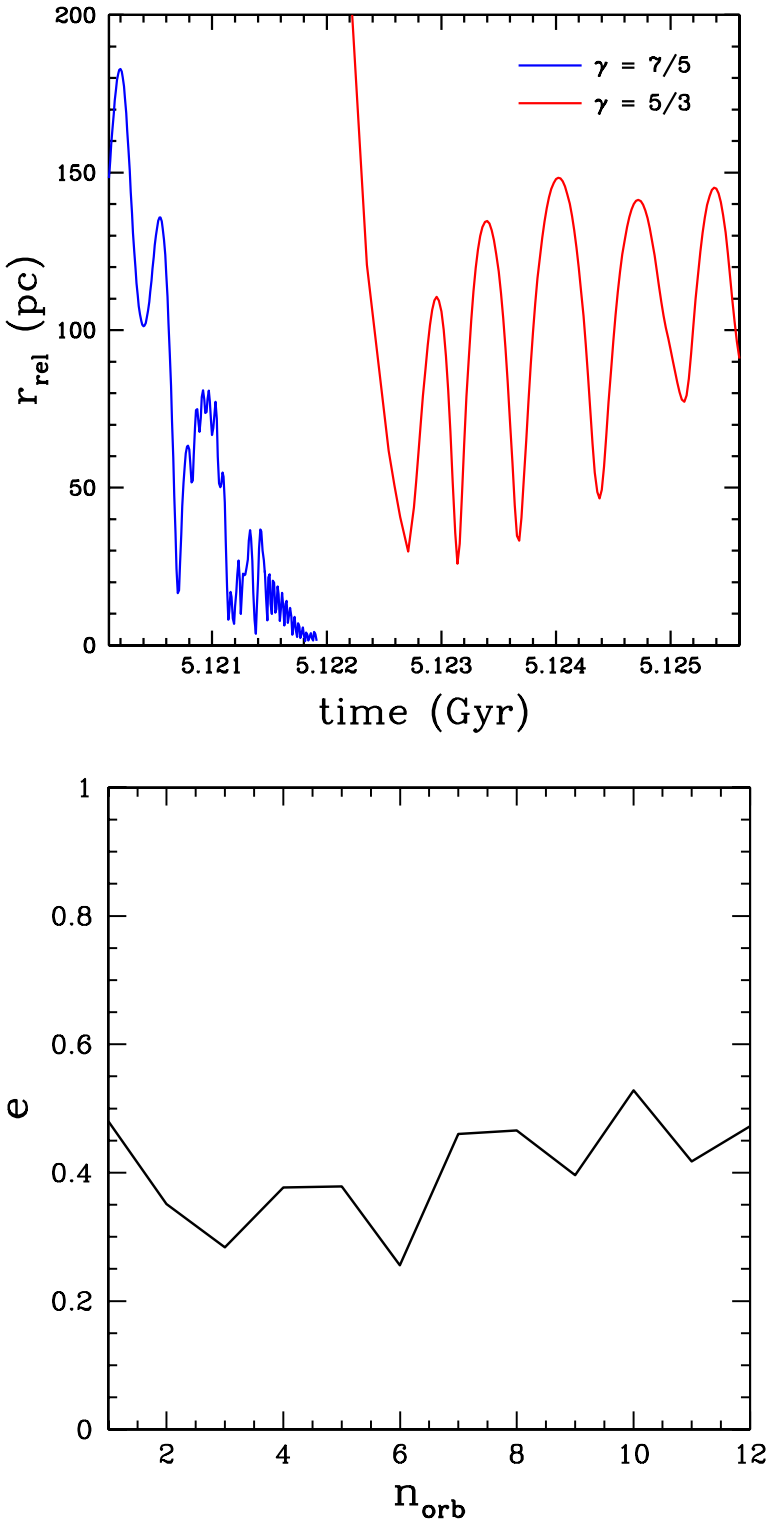

Figure S4. Top: Orbital evolution of the binary supermassive black holes. The blue line shows the relative distance as a function of time for the pair in the $\gamma = 7/5$ simulations, as in Figure 2 of the Report, while the red line shows it for the $\gamma = 5/3$ simulation (see section 2.1). Bottom: Evolution of the eccentricity of the pair of SMBHs as a function of the number of orbits performed in the nuclear disk in the $\gamma = 7/5$ simulation. The binary forms after about eight orbits. The time spanned by the orbits corresponds to that in the inset of Figure 2 of the Report.

2 Supporting Online Text

2.1 Effects of thermodynamics on the sinking of the SMBHs

We tested how a smaller degree of dissipation affects the structure and dynamics of the nuclear region by increasing γ to $5/3$. This would correspond to a purely adiabatic gas, or equivalently it corresponds to the assumption that radiative cooling is completely negligible. The radiative feedback from an active galactic nucleus (AGN) is a good candidate for a strong heating source that the models on which we based our prescription for thermodynamics described in the previous section do not take into account($S31$, $S32$). An AGN would not only act as an additional source of radiative heating but would also increase the turbulence in the gas by injecting kinetic energy in the surrounding medium, possibly suppressing gas cooling($S37$, $S38$). Even before the two galaxy cores merge, when they are still a few kpc away, a mild gas inflow collects more than $10^8 M_\odot$ within a few hundred parsecs from the black holes. The gas is already arranged in a disk-like structure, which is highly tidally distorted and presents inward radial motions. Therefore, there is room to imagine that significant gas accretion might take place before the merger is completed, turning one or both the two black holes into an AGN.

We have run another refined simulation with $\gamma = 5/3$ to explore this extreme situation. In this case we find that a turbulent, pressure supported cloud of a few hundred parsecs arises from the merger rather than a disk. The mass of gas is lower within 100 pc relative to the $\gamma = 7/5$ case because of the adiabatic expansion following the final shock at the merging of the cores. The nuclear region is still gas dominated, but the stars/gas ratio is > 0.5 in the inner 100 pc. The black hole pair does not form a binary due to inefficient orbital decay, and maintains a separation of $\sim 100 - 150$ pc (Figure S4) well after they have formed a binary in the $\gamma = 7/5$ case. The gas is hotter and more turbulent; the sound speed $v_s \sim 100$ km/s and the turbulent velocity $v_{\rm turb} \sim 300$ km/s become of the same order of $v_{\rm bh}$, the velocity of the black holes,

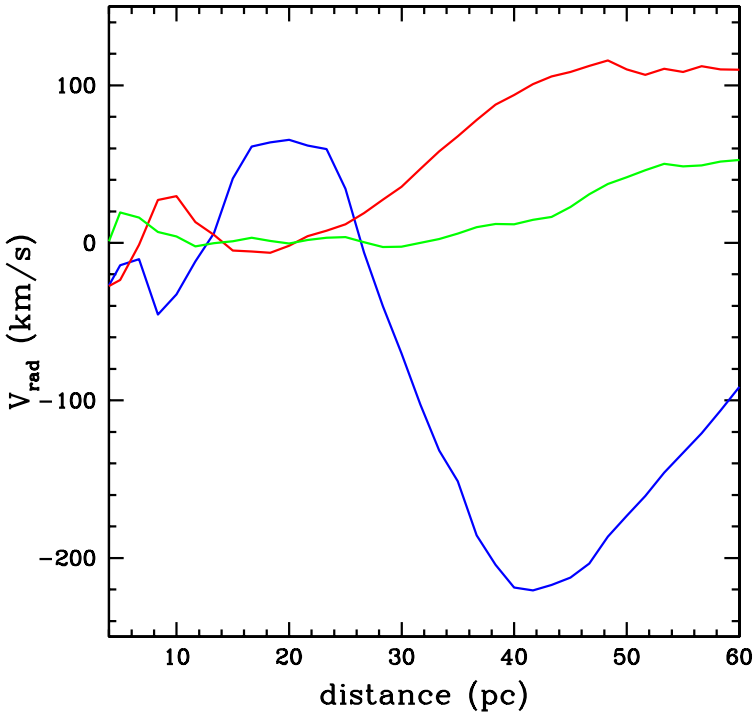

Figure S5. Radial velocities within the nuclear disk ($\gamma = 7/5$) starting at $t = 5.1218$ Gyr (blue line), and then after another 10^5 years (red line) and 2×10^5 years (green line). Remarkable inflow and outflow regions are the result of streaming motions within the bar and spiral arms arising in the disk during the phase of non-axisymmetric instability sustained by its self-gravity At later times the instability saturates due to self-regulation and the radial motions also level down (green line).

and the density around the black holes is ~ 5 times lower than in the $\gamma = 7/5$ case. The lower density, and to a minor extent the fact that the motion of the two black holes occurs in a transonic rather than in a supersonic regime greatly reduce the drag due to the gas (see below).

A strong form of AGN feedback which can shut off cooling at galactic as well as at cluster scales has been sometimes advocated to stop the cooling flow in clusters, create entropy cores and, in general, reduce the overcooling problem at large scales$(S39, S40)$. Given the discovered sensitivity to the value of γ, it would appear that a scenario in which black holes rapidly form a binary and eventually later coalesce owing to the drag provided by the gas requires that models for AGN feedback be effective on the large scale and simultaneously have negligible thermodynamical effects at small scales. This might indeed be a more general requirement if one has to preserve the ubiquitous nuclear disk-like structures seen in many merger remnants (see below section 2.2). Indeed, previous works that included a prescription for AGN feedback in galaxy merger simulations similar to ours$(S37, 38)$ find that feedback affects strongly the

thermodynamics of the gas in the nuclear region only $> 10^8$ years after the merger is completed.

As briefly mentioned in the Report, we have attempted a simple calculation of the accretion rate of the black holes and of their released energy output assuming Bondi-Hoyle spherical accretion of the gas within twice the softening of the black holes, following the scheme adopted in $(S37, S38)$. We have neglected the motion of the black holes relative to the surrounding gas since these move on orbits corotating with the disk (hence there is nearly no net relative motion between the gas and the holes). In addition, we have assumed that the radiative emission is Eddington limited and occurs with an efficiency of 10% (indeed we find that they can sustain a mean accretion rate of $0.05 M_\odot$/yr, slightly below Eddington) and would radiate an amount of energy nearly comparable to the internal energy of the gas (the sum of turbulent, rotational and thermal energy) over the time comprised between the formation of the nuclear disk and the formation of the binary. The latter result is obtained if all the radiated energy goes into heating the surrounding gas isotropically, neglecting radiative losses or hydrodynamical instabilities at the interface between different phases, such as Kelvin-Helmoltz or Rayleigh-Taylor instabilities, that can convert thermal energy into turbulent energy. Isotropic heating was also assumed in $(S37, S38)$, who indeed matched the $M - \sigma$ relation by depositing only 5% of the emitted energy into heating of the gas. If we make the same assumption here then the total radiated energy over the same timescale is smaller than the internal energy of the gas by more than a factor of 50. This leads us to conclude that the radiative heating from the SMBHs should not affect significantly the thermodynamics of the gas and thus its equation of state. However, if the black holes begin accreting earlier on, when the two galaxy cores have not merged yet, the integrated energy output until the binary forms can be much larger and could affect the thermodynamics of the newly formed nuclear disk. Indeed once the black holes become active they would be able to accrete and emit at the Eddington limit for at least a Salpeter time, which

is 4×10^7 yr, a timescale almost 100 times longer than the binary formation timescale (there is indeed enough gas in the nuclear region to sustain an even more prolonged accretion, albeit below Eddington). While gas accretion should be more effective, and thus the assumption that emission occurs at the Eddington limit more sensible, when the nuclear disk has already formed simply because the gas has larger inward radial motions and thus should feed the black holes more efficiently (see also section 2.2) only higher resolution calculations capable of studying in detail the dynamics of the gas near the holes will be able to address the issue of when accretion becomes significant, and if and when it can produce a significant energetic feedback on the nuclear disk. Furthermore, additional test runs that we have performed (without black holes) show that if the equation of state becomes stiffer ($\gamma = 5/3$ instead of $\gamma = 7/5$) only *after* the merger is completed, the nuclear disk structure is barely affected (this would correspond to the case in which the SMBHs become active only after the formation of the nuclear disk). Therefore the timing of accretion during the merger is a crucial aspect that will have to be explored by future work. Section 2.2 will briefly discuss how the structure of the inner gaseous distribution in runs with different values of γ compares with the observations of the nuclear regions of merger remnants.

In the $\gamma = 5/3$ case the black holes could still decay and form a binary as a result of the interaction with the stellar background. Since the resolution of the stellar background in the simulations is likely inadequate to assess directly the effect of dynamical friction, we calculated the dynamical friction timescale in a collisionless background analytically$(S41)$ using

$$\tau_{DF} = 1.2 \frac{V_{cir} r_{cir}^2}{[GM_{bh}/\mathrm{e}] \ln(M_{sd}/M_{bh})} \varepsilon^{0.4} \qquad (1)$$

where $V_{\rm cir}$ and $r_{\rm cir}$ are, respectively, the initial orbital velocity and the radius of the circular orbit with the same energy of the orbit of the black holes in the simulation, and ε is the circularity

of the orbit ($\varepsilon = J(E)/J_{cir}(E)$, where $J(E)$ is the angular momentum of the orbit as a function of its orbital energy E and $J_{circ}(E)$ is the angular momentum of a circular orbit having the same orbital energy E, so that $\varepsilon = 0$ corresponds to a radial orbit and $\varepsilon = 1$ corresponds to a circular orbit), M_{sd} is the sum of the dark matter and stellar mass within r_{cir}. We calculate the decay time starting from when the two black holes are 100 pc apart, namely at the periphery of the nuclear disk, just after the merger. Drawing the numbers from the simulation we set $r_{\rm cir} = 100$ pc, $V_{\rm circ}$= 200 km/s, $\varepsilon = 0.5$, $M_{\rm bh} = 2.4 \times 10^6 M_\odot$ and $M_{\rm sd} = 5 \times 10^8 M_\odot$. We find that timescales for dynamical friction timescale in a collisionless background are 5×10^7 yr and 3×10^7 in the $\gamma = 5/3$ and $\gamma = 7/5$ case, respectively (the shorter timescale in the $\gamma = 7/5$ case is due to the fact that the stars and halo adiabatically contract more in response to the higher gas mass concentration, hence $M_{\rm sd}$ is higher). In comparison, the binary formation timescale in the $\gamma = 7/5$ simulation is only 5×10^5 years.

Equation 1 was derived for an isothermal sphere. The stellar and dark matter distribution are indeed only mildly triaxial within a few hundred parsecs from the center ($c/a > 0.7$, where c is the semi-minor axis and a the semi-major axis of the mass distribution) and the total profile is extremely close to that of an isothermal sphere($S8$). The fact that the merger remnant is not far from spherical confirms the predictions of larger-scale simulations regarding the effect of gas cooling on the structure of the global potential($S42, S43$). Note that equation actually yields a lower limit to the dynamical friction timescale since close to parsec scales, as the binary becomes hard, evacuation of the stellar background due to three-body encounters will begin, and the efficiency of the sinking process will be greatly reduced. Whether sinking will continue and eventually lead to coalescence of the two holes is uncertain in this case given the fact that the gas does not play an important role. Centrophilic orbits in triaxial systems would help in refilling the loss cone, and could in principle bring the black holes down to the distance where gravitational waves would take over($S44$). However, as we just mentioned, the structure

of the stellar core is only mildly triaxial. Further investigation with simulations having higher resolution in the collisionless component is needed. The $\gamma = 5/3$ run was stopped 5×10^6 years after the merger of the gaseous cores is completed. Once again, the fact that there is no evidence that the holes are sinking until the end is likely due to insufficient mass and force resolution in the collisionless background that does not allow to resolve dynamical friction properly$(S45)$ (as we will explain in the remainder of this section the gas contributes little to the drag in this case).

We also compared our results with the expected dynamical friction timescale due to the gaseous background. In the run with $\gamma = 7/5$ the gas is distributed in a disk rather than in an isothermal sphere. Since the disk thickness is > 10 times the black hole gravitational softening and owing to the fact that the density profile of the disk can be roughly approximated with a power law with an index close to 2 (except at the center where it becomes steeper) we are allowed to use eq. (1) to obtain a rough estimate. As previously shown$(S28)$, analytical predictions$(S36)$ can overestimate the drag in the supersonic regime by a factor ~ 1.5. In the $\gamma = 7/5$ case the regime is mildly supersonic and the analytical formula should yield the correct prediction. In this case the drag is ~ 2.3 time stronger than in the corresponding collisionless case$(S28)$. This is fairly consistent with our results. Indeed, formula (1) with a reduction of a factor of 2.3 would give $2.3 \sim 10^6$ yr if we set $M_{gas} = M_{sd}$, the gas mass being about 20 times more than the mass in stars. This timescale has to be compared with that measured in the simulation, 5×10^5 yr (we recall that the gas profile is steeper than r^{-2} near the center, therefore it is not surprising that the decay is actually faster).

Despite the apparent agreement with the analytically estimated drag we note that the orbital dynamics of the two black holes might be affected by more than just the gravitational wake. Indeed the disks show strong , highly dynamical non-axisymmetric features such as spiral arms (see next section); in the analogous, well-studied case of planet migration orbital decay is well

described by torques exerted onto the target body by the spiral modes and its efficiency depends on the location of resonances between the orbital motion and the spiral pattern that extract or deposit angular momentum($S46$). The latter description of the orbital decay might be more appropriate here rather than just considering the effect of the gravitational wake (see also the discussion on the orbital eccentricity below)

The drag drops rapidly by an order of magnitude approaching the subsonic regime($S20$); this coupled with the fact that M_{gas} is a factor of 5 lower in the $\gamma = 5/3$ would give a drag 50 times smaller in the latter case, explaining why the orbital decay provided by the gas is so inefficient in such conditions.

In summary, in the $\gamma = 7/5$ run the sinking timescale due to the gas is much shorter than that due to the stellar background because of the combination of (1) the fact that gas densities are much higher than stellar densities in the center and (2) the fact that in the supersonic regime the drag in a gaseous background is stronger than that in a stellar background with the same density. Adding star formation is unlikely to change this conclusion. In fact the low-resolution galaxy mergers simulations yield a starburst timescale of 5×10^7 yr. During this time, which is much longer than the binary formation timescale, half of the gas in the nuclear disk is turned into stars. Instead, in the $\gamma = 5/3$ stars and gas would contribute to the drag in a comparable way as the black holes begin to sink but since the sinking timescale is much longer and comparable with the star formation timescale the overall orbital evolution will be dictated by the stars rather than by the gas.

There are, however, some caveats in our argument regarding the role of star formation in the $\gamma = 7/5$ case. First, the starburst timescale is based on the low resolution merger simulations. Had we included star formation in the refined simulations we would have probably found shorter timescales locally since these simulations are capable of resolving much higher densities and the star formation rate depends on the local gas density. Second, one might wonder how the

inclusion of feedback from star formation, which was neglected in the low resolution merger simulations, would affect gas properties and, eventually, the orbital decay of the black holes. As for the first issue, we can obtain a rough estimate of how short the star formation timescale can be in the following way. We note that in the nuclear disk most of the gas is at densities above 100 atoms/cm^3. At these densities molecular hydrogen formation is efficient $(S47)$. Let us then make the rather extreme assumption that all the gas in the disk is molecular and readily available for star formation. Then, let us simply assume that molecular gas will be turned into stars on the local orbital timescale. Star formation in molecular clouds is rather inefficient, and typically 30% of the dense, molecular gas only is converted into stars, possibly because internal turbulence in the clouds prevents them from collapsing altogether $(S48)$. Therefore let us write the star formation rate in the nuclear disk as a whole as $dM_*/dt = 0.3 \times M_{gas}/T_{orb}$, where $T_{orb} = 10^6$ years, the orbital time at the disk half mass radius, 25 pc, and $M_{gas} = 3 \times 10^9 M_\odot$. The resulting star formation rate is $900 M_\odot$/yr , about 25 times higher than that estimated in the low-res simulations. Nonetheless, even with such high star formation rate less than 1/5 of the gas in the disk, $4.5 \times 10^8 M_\odot$, would be converted into stars during the time required for the black holes to sink and bind in the nuclear disk (5×10^5 years). Regarding the issue of feedback, radiative feedback from stars is implicitly included in our choice of the equation of state in the $\gamma = 7/5$ case (see above), but feedback from supernovae explosions is not taken into account. However, supernovae feedback would contribute to both heating the gas and increasing its turbulence, which should go in the direction of decreasing the star formation rate and therefore strengthening our previous argument concerning the role of star formation. Moreover, while it will have remarkable effects on the multi-phase structure of the gas $(S34 - S35)$, it should not have a major impact on the energetics of the disk in the $\gamma = 7/5$ case. In fact, assuming a star formation rate of $900 M_\odot/yr$ and a Miller-Scalo initial stellar mass function we obtain that supernovae should damp $\sim 4 \times 10^{51}$ erg/yr (7×10^{48} erg per solar mass

of stars formed) into the surrounding gas, corresponding to $\sim 2 \times 10^{57}$ erg damped during the binary formation timescale, 5×10^5 yr. This is about 50% smaller than the internal energy of the gas in the nuclear disk (the sum of turbulent, rotational and thermal energy). However, since the decay of the black holes will be sensitive to changes in the local gas density along their orbit, only future calculations that incorporate directly the effects of star formation and supernovae explosions will probably find quantitative differences relative to our simple thermodynamical model.

We note the black holes sink on an eccentric orbit in the nuclear disk (see above). We tracked the evolution of the eccentricity after the two cores merge and the holes are embedded in a single disk and found that despite fluctuations the eccentricity e after about 10^6 yr is roughly identical to its initial value, $e \sim 0.5$ (Figure S4). Only in the initial phase of the decay we do signs a tendency of circularization. This is different from what found in $(S30)$, who measured fast circularization of for binaries of SMBHs evolving in equilibrium nuclear disks. A caveat in the comparison is that we can only follow a few orbits once the binary is formed in the refined simulations. Nevertheless, a tendency towards circularization is clear already during the first few orbits in $(S30)$, contrary to what we find here. The reason for this difference is not clear but it is probably related to differences in the structure of the nuclear disk. The disk in the refined simulation has a much stronger spiral pattern than that in $(S30)$ due to its much higher self-gravity, having a mass 30 times higher. Analytic calculations of tidal torques in the context of planet migration $(S49)$ have shown that a massive body moving in an eccentric disk is characterized by an orbit whose eccentricity is comparable to the degree of non-axisymmetry of the disk. Such calculations considered a simple m=1 spiral mode superimposed on the disk potential as the source of the "eccentricity" of the disk (the mode is treated as a forcing term in the equations of motion) but the results should be quite general in a qualitative sense. The consequence is that a black hole in a strongly non-axisymmetric disk should move on a more

eccentric orbit relative to the case of a mildly axisymmetric disk, and that this tendency for the natural orbit (in the sense that it is the natural solution of the equations of motion) to be eccentric should counteract the tendency of dynamical friction to circularize the orbit as the black holes decay. The net outcome will depend on how the structure of the nuclear disk evolves with time. This is an important issue that warrants further investigation because the coalescence time of the binary in the gravitational radiation dominated phase depends on its orbital eccentricity.

Finally, the last stage of the refined simulations provides the initial conditions for future models that will eventually follow the hardening of the binary below parsec scales. These future calculations will be able to show whether the last parsec problem can be overcome in the nuclei of merger remnants with gas, as suggested by simulations of binary SMBHs embedded in equilibrium nuclear disks $(S20, S28 - S30)$. The binary should continue to sink as a result of gas drag . Its sinking rate, however, will strongly depend on the dynamics and thermodynamics of the disk at scales below the resolution of the refined simulations. The properties of the gas below one parsec will determine whether a gap will be opened by the binary, slowing down significantly albeit not stopping its orbital decay, or whether the holes will sink at a faster rate as a result of torques by the asymmetries in the mass distribution surrounding the two holes $(S28 - S30)$. Whether or not an appreciable fraction of the gas will be converted into stars by the time the separation of the binary has fallen below a parsec will also have an impact since, for instance, the conditions for gap formation will depend on the local gas density and the overall sinking rate might have a non-negligible contribution from the stars.

2.2 Structure and kinematics of the nuclear disks

The nuclear disk produced in the $\gamma = 7/5$ case is highly turbulent. The source of turbulence are the prominent shocks generated as the cores merge and the persistent non-axisymmetric structure sustained by the self-gravity of the disks after the merger is completed$(S34, S35)$.

The perturbation due to the binary black holes is a negligible effect since their mass is about 10^3 times smaller than the mass of the disk (we tested this by restarting a simulation after removing the black holes once the merger is completed). The degree of turbulence, of order $50 - 100$ km/s as measured by the radial velocity dispersion, is comparable to that of observed circumnuclear disks($S33, S47$). The disk is composed by a very dense, compact region of size about 25 pc which contains half of its mass (the mean density inside this region is $> 10^5$ atoms/cm^3). The outer region instead, from 25 to 75-80 pc, has a density 10-100 times lower, and is surrounded by even lower density rotating rings extending out to a few hundred parsecs. The disk scale height also increases from inside out, ranging from 20 pc to nearly 40 pc. The volume-weighted density within 100 pc is in the range $10^3 - 10^4$ atoms/cm^3, comparable to that of observed nuclear disk ($S33$). This suggests that the degree of dissipation implied by our equation of state is a reasonable assumption despite the simplicity of the thermodynamical scheme adopted.

The rotating, flattened cloud produced in the $\gamma = 5/3$ is instead more turbulent and less dense than observed circumnuclear disks in merger remnants. The mean velocity dispersion measured within 100 pc is about 300 km/s, higher than the mean rotational velocity within the same radius, which is ~ 250 km/s. This suggests that the $\gamma = 5/3$ simulation does not describe the typical nuclear structure resulting from a dissipative merger, The strong spiral pattern in the disk produces remarkable radial velocities. Since spiral modes transfer angular momentum inwards and mass outwards($S52, S53$) , strong inward radial velocities are present. The amplitude of radial motions evolves with the amplitude of the spiral pattern, in the sense that radial motions decline as the spiral arms weaken over time. Just after the merger, when non-axisymmetry is strongest, radial motions reach amplitudes of ~ 100 km/s (Figure S5). This phase lasts only a couple of orbital times, while later the disk becomes smoother as spiral shocks increase the internal energy which in turn weakens the spiral pattern. Inward radial

velocities of order $30 - 50$ km/s are seen for the remaining few orbital times during which we are able to follow the system (Figure S5). Such velocities are comparable to those recently seen in high resolution observations of the nuclear disk of nearby Seyfert galaxies$(S54)$. As the gas reaches down to a few parsecs from the center its radial velocity diminishes because one approaches the limits of the gravitational force resolution in the simulation (~ 2 pc). Therefore the fact that there is almost no net radial velocity within a few parsecs from the center (Figure S5) is an artifact of the limited resolution. In addition, in this innermost region the gas is so dense ($\rho > 10^5$ cm^{-3}) that our equation of state breaks down, since a lower γ, close to the isothermal value, would be more appropriate (see section 1.4). A higher dissipation rate likely means the gas inflow rate in the innermost region of the disk will be higher than the one seen in the current simulations$(S55)$. If we assume that speeds of $30 - 50$ km/s can be sustained down to scales of a few parsecs, $> 10^8 M_\odot$ of gas could reach parsec scales in about 10^5 yr. The latter timescale is much smaller than the duration of the starburst, and therefore such gas inflow should develop in a similar way even when star formation is taken into account. The inflow is also marginally faster than the decay timescale of the binary SMBH measured in the simulations, which is $\sim 5 \times 10^5$ years. Presumably some of this gas could be intercepted by the two SMBHs as they are spiraling down (the relative velocities between the gas and the black holes are small since the SMBHs are always corotating with the nuclear disk), but the higher dissipation rate expected near the central, denser regions might increase the magnitude of the drag due to the gas in reality and bring the sinking time of the binary very close to the gas inflow timescale. In the latter case the two SMBHs could undergo massive accretion, and probably become active while they are sinking. Only future simulations that include a realistic treatment of the gas thermodynamics at all scales will be able to study gas accretion and orbital decay simultaneously.

Our single-phase simulations seem to describe reasonably well the average properties of

observed nuclear disk because they capture the thermodynamics of the low density, pressurized medium that has the largest volume filling factor $(S33)$. Yet they do not model directly the molecular gas, which will have temperatures of order 100 K, much lower than the effective temperature produced by our equation of state, and comprises most of the gas mass in observed nuclear disks $(S33)$. The dense molecular phase would be better described as an ideal gas with $\gamma = 1$ or lower (see 1.4). While a model of the multi-phase interstellar medium in the disk should be the ultimate goal for future simulations, one could also design an intermediate scheme in which the equation of state (in particular γ) changes as a function of density, as done in simulations of molecular cloud collapse $(S26)$. If a large fraction of the gas has a much softer equation of state compared to the $\gamma = 7/5$ runs a much denser and thinner disk will likely form. We performed a simulation that adopts an isothermal equation of state ($\gamma = 1$) in the refined part of the calculation and indeed the resulting disk has a mass comparable to that in the previous calculations but a scale height of only ~ 5 pc, which would probably shrink even further with a higher spatial resolution. The sound speed is only 10 km/s compared to 60 km/s in the $\gamma = 7/5$ case, and turbulence is also much weaker. The disk is violently gravitationally unstable, with dense rings and arms, which would likely fragment with a smaller softening. The simulation was stopped after the merger because the very high densities at the center prevented an efficient integration. However, the cores merged faster than in the $\gamma = 7/5$ case and we expect the black holes would also sink faster based on the results of previous work $(S28)$ that found how the orbital decay is faster when the gas has a higher density and/or has a lower sound speed, even in the case in which the disk is significantly clumpy. In reality the nuclear region will have the global properties, especially the global energetics, of our $\gamma = 7/5$ simulation, while locally the densest gas will have properties closer to that of the isothermal test run. Such a complex multi-phase structure is predicted by simulations of self-gravitating turbulent disks $(S34 - S35)$.

References and Notes

S1. Wadsley, J., Stadel, J., & Quinn, T., *New Astr*., **9**, 137 (2004)

S2. Barnes, J., & Hut, P., *Nature*, **324**, 446 (1986)

S3. Gingold, R.A. & Monaghan, J.J., *Mon. Not. R. Astron. Soc.*, **181**, 375 (1977)

S4. Monaghan, J.J., *Annual. Rev. Astron, Astrophys*, **30**, 543 (1992)

S5. Barnes, J., *Mon. Not. R. Astron. Soc.*, **333**, 481 (2002)

S6. Springel, V. and Hernquist, L., *Mon. Not. R. Astron. Soc.*, **333**, 649 (2002)

S7. Balsara, D.S., *J.Comput. Phys.*,121, 357 (1995)

S8. Kazantzidis, S., Mayer, L., Colpi, M., Madau, P., Debattista, V., Quinn, T., Wadsley, J. & Moore, B., *Astrophys. J.*, **623**, L67 (2005)

S9. Katz, N. *Astrophys. J.*, **3**91, 502 (1992)

S10. Governato, F., Mayer, L., Wadsley, J., Gardner, J. P., Willman, B., Hayashi, E., Quinn, T., Stadel, J.& Lake, G, *Astrophys. J.*, **607**, 688 (2004)

S11. Hernquist, L., *Astrophys. J. Supp.*, **86**, 389 (1993)

S12. Springel, V. & White, S.D.M., *Mon. Not. R. Astron. Soc.*, **307**, 162 (1999)

S13. Mo, H. J., Mao, S., White, S. D. M., *Mon. Not. R. Astron. Soc.*, **295**, 319 (1998)

S14. Navarro, J. F., Frenk, C. S. & White, S. D. M., *Astrophys. J.*, **462**, 563 (1996)

S15. Kazantzidis, S., Mayer, L., Mastropietro, C., Diemand, J., Stadel, J., & Moore, B., *Astrophys. J.*, **608**, 663 (2004)

S16. Klypin A., Zhao H. & Somerville R. S., *Astrophys. J.*, **573**, 597 (2002)

S17. Blumenthal, R.G., Faber, S.M., Flores, R., & Primack, J.R., *Astrophys. J.*, **3**01, 27 (1986)

S18. Khochfar, S. & Burkert, A., *Astron. Astrophys.*, **445**, 403 (2006)

S19. Kaufmann, T., Mayer, L., Wadsley, J., Stadel, J. & Moore, B., *Mon. Not. R. Astron. Soc.*, **370**, 1612 (2006)

S20. Escala, A., Larson, R. B., Coppi, P. S., & Mardones, D., *Astrophys. J.*, **607**, 765 (2004)

S21. Bromm, V. & Loeb, A., *Astrophys. J.*, **596**, 34 (2002)

S22. Kitsionas, S. & Whitworth, S., *Mon. Not. R. Astron. Soc.*, **330**, 129 (2002)

S23. Steinmetz, M. & White, S.D.M., *Mon. Not. R. Astron. Soc.*, **288**, 545 (1997)

S24. Bate, M. & Burkert, A., *Mon. Not. R. Astron. Soc.*, **288**, 1060 (1997)

S25. Nelson, A.F., *Mon. Not. R. Astron. Soc.*, **373**, 1039 (2006)

S26. Bate, M.R., Bonnell. I.A., & Bromm, V., *Astrophys. J.*, **336**, 705 (2002)

S27. Mayer, L., Kazantzidis, S., Madau, P., Colpi, M., Quinn, T., & Wadsley, J., 2006b, Proc. Conf. Relativistic Astrophysics and Cosmology - Einstein's Legacy (astro-ph/0602029).

S28. Escala A., Larson, R. B., Coppi, P. S. & Mardones, D., *Astrophys. J.*, **630**, 152 (2005)

S29. Dotti, M., Colpi, M. & Haardt, F., *Mon. Not. R. Astron. Soc.*, **367**, 103 (2006)

S30. Dotti, M., Colpi, M., & Haardt, F., & Mayer, L., *Mon. Not. R. Astron. Soc.*, in press (astro-ph/0612505)

S31. Spaans, M. & Silk, J.,*Astrophys. J*, **538**, 115 (2000)

S32. Klessen, R.S., Spaans, M., Jappsen, A., *Mon. Not. R. Astron. Soc.*, **374**, L29 (2007)

S33. Downes, D. & Solomon, P. M., *Astrophys. J.*, **507**, 615 (1998)

S34. Wada, K., *Astrophys. J.*, **559**, L41 (2001)

S35. Wada, K. & Norman, C., *Astrophys. J*, **566**, L21 (2002)

S36. Ostriker, E., *Astrophys. J.*, **513**, 252 (1999)

S37. Springel, V., Di Matteo, T., & Hernquist, L.*Mon. Not. R. Astron. Soc.*, **361**, 776 (2005)

S38. Di Matteo, T., Springel, V. & Hernquist, L., *Nature* **7026**, 604 (2005)

S39. Croton, D. J. *et al.*, *Mon. Not. R. Astron. Soc.*, **365** 11 (2006)

S40. Bower, R.G., *et al.*, *Mon. Not. R. Astron. Soc.*, **370**, 645 (2006)

S41. Colpi, M., Mayer, L. & Governato, F., *Astrophys. J.*. **5**25, 720 (1999)

S42. Dubinski, J.,*Astrophys. J.*, **431**, 671 (1994)

S43. Kazantzidis, S., Kravtsov, A.V., Zentner, A.R., Allgod, B., Nagai, D. & Moore, *Astrophys. J.*, **6**11, L73-L76 (2004)

S44. Beczik, P., Merritt, D., Spurzem, R. & Bischof, H.P., *Astrophys. J.*, **641**, L21 (2006)

S45. Weinberg, M. & Katz, N., *Mon. Not. R. Astron. Soc.*, **375**, 425 (2007)

S46. Papaloizou, J.C.B., & Larwood, J.D., *Mon. Not. R. Astron. Soc.*, **(315**, 823 (2000)

S47. Schaye, J. *Astrophys. J.*, **809**, 667 (2004)

S48. Li, Y., Mac Low, M.M., & Klessen, R.S., *Astrophys. J.*, **626**, 823 (2005)

S49. Papaloizou, J.C.B., *Astron. Astrophys.*, **388**, 615, (2002)

S50. Greve, T.R., Papadopoulos, P.P., Gao, Y., & Radford, S.J.E., submitted to Astrophys. J. (2006) (astro-ph/0610378)

S51. Laughlin, G., Korchagin, V. & Adams, *Astrophys. J.*, **477**, 410 (1997)

S52. Mayer, L., Quinn, T., Wadsley, J. & Stadel, J.,*Astrophys. J.*, **609**, 1045 (2004)

S53. Fathi, K. et al. *Astrophys. J.*, **641**, L25 (2006)

S54. Escala, A., *Astrophys. J.*, **648**, L13 (2006)